Fall 2015

Performance metrics for powder feeder systems in additive manufacturing

Venkata Sivaram Bitragunta

PERFORMANCE METRIC FOR POWDER FEEDER SYSTEMS IN ADDITIVE MANUFACTURING

by

VENKATA SIVARAM BITRAGUNTA

A THESIS

Presented to the Graduate Faculty of the

MISSOURI UNIVERSITY OF SCIENCE AND TECHNOLOGY

In Partial Fulfillment of the Requirements for the Degree

MASTER OF SCIENCE

in

MANUFACTURING ENGINEERING

2015

Approved by

Dr. Frank Liou, Advisor
Dr. Joseph Newkirk
Dr. Heng Pan

ABSTRACT

In blown powder Direct Metal Deposition (DMD) process, parts are built by adding metal powder on the melt pool created by the laser system. At low feed rates powder feeder systems have perturbations. The study focused on relationship between the perturbation frequencies by inherent powder feeder designs and its impact on deposition quality. Performance metric determine the relation between perturbations in the powder flow and quality of the deposit. To determine performance metric, various powder feeder designs were analyzed. Perturbation frequencies were introduced to the disk feeder design. The quality of the deposit was determined by the surface roughness of the deposit. A laser displacement sensor was used to measure the surface roughness of the deposits. Experiments were carried out to determine the significance between measured surface roughness values of the deposits over theoretically calculated performance metric values. Validation tests were done to compare the data fit. The wheel feeder and newly developed disk feeder were compared for deposit quality. The results showed better performance metric for the disk feeder system under the same process parameters. Based on this metric, a feeder system can be chosen in the future to produce Functionally Graded Materials (FGM).

ACKNOWLEDGMENTS

I would like to express my most sincere gratitude to my research and academic advisor, Professor Frank W. Liou, for his guidance, encouraging advice, inspiring discussions, great patience, and financial support. I would not have reached this point without his support. I would also like to thank Dr. Joseph W. Newkirk and Dr. Heng Pan for serving on my thesis committee. They provided insightful comments and invaluable assistance that undoubtedly contributed to the success of this work.

I am grateful to Todd Sparks for sharing ideas and conducting experiments in LAMP lab. I am also thankful for having had the opportunity to work with Connor Coward, Sreekar Karnati, George Holmes, and Maxwell Mulholland of Laser Aided Manufacturing Process (LAMP) lab. I must acknowledge to the academic and financial support I received from the Department of manufacturing engineering. This work would not have been possible without this support. I sincerely thank Mr. Bullock, Brain E. of the machine shop at the mechanical engineering department (MAE), Missouri University of Science & Technology.

Last but not the least, I would like to thank my parents, for the immeasurable care, support and love they always have.

TABLE OF CONTENTS

Page

LIST OF ILLUSTRATIONS

LIST OF TABLES

Table Page

1. INTRODUCTION

1.1. DIRECT METAL DEPOSITION PROCESS

The Direct Metal Deposition (DMD) process is an additive manufacturing process. Parts are built on a layer by layer fashion by adding metal powder to the melt pool created by the laser on a substrate. DMD process has the capability to produce fully dense functional parts directly from a CAD model. It is suitable to build parts with complex shapes that are hard to manufacture using traditional manufacturing methods. It is also utilized in the area of repair and modify metallic components.

1.2. POWDER FEEDER SYSTEMS

The DMD process requires a stable and consistent powder delivery system to maintain quality deposits. The study on the design of powder feeder systems for the DMD process helped to control the quality of the part built by understanding the critical design parameters. Commercially available powder feeder systems are either custom made for a particular DMD process or designed for high mass flow rate applications like laser cladding or thermal spraying. Figure 1.1 illustrates typical powder feeder systems used for the additive manufacturing process. The carrier gas is used as a utility in the DMD process. Powder from the hopper is delivered at a consistent rate using the carrier gas as the transport medium. The change of powder flow depends on the feeding system. For the DMD process, low feed rates are a top priority.

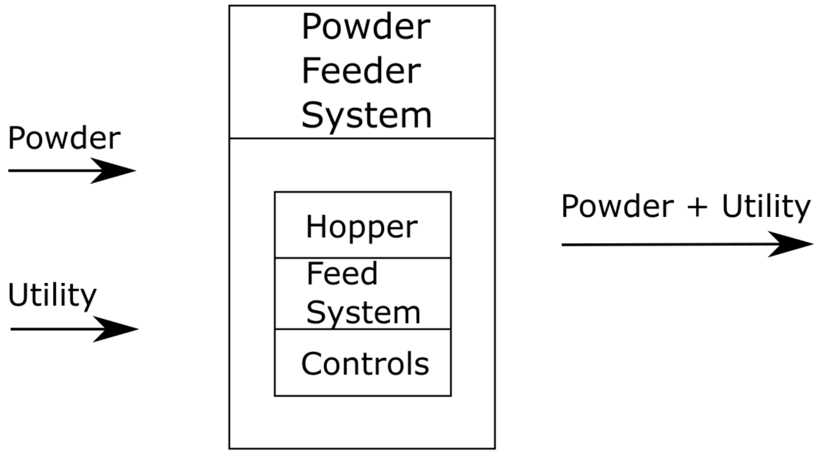

Figure 1.1. A Schematic Representation of Process Flow and Critical Components of Powder Feeder Systems Used in Blown Powder Direct Metal Deposition

1.3. DEVELOPMENT OF POWDER FEEDER SYSTEMS

Powder feeder systems are consistently evolving, with more interesting and challenging powders to feed. As additive manufacturing processes are being applied to many new possibilities in recent years, there has been a constant thrust to support these opportunities. The literature review discusses various feeding systems developed for powder feeders in the DMD process.

In 1980 Gullett[5] worked to develop low feed rate feeders. They built a new fluidization feeder design that feed agglomerative particles. Later Todd Francis [3] worked to design a fluidized bed feeder. Conveying feeding design was developed by Todd Francis [2] using a carrier gas. The powder stored in hoppers under vibration moves around the spinning wheel. It is then supplied to the feeding system by a carrier gas. Most of this work was to agglomerate powders.

Chianrabutra [1] and others worked to develop a feeding mechanism for dry powders. Matsusaka [9] investigated the micro feeding of fine powders in a capillary tube. Takano and Tomikawa [12] developed feeding devices based on the excitation of a progressive wave in an ultrasonic transmission line. Li [8] used an ultrasonic-based micro powder feeding mechanism to form thin patterns of powders on a substrate. The powders were subsequently sintered by a laser beam. Kumar [6] examined the concept of multiple dry powder deposition under gravity flow including low gas pressure assisted flow and vibration-assisted flow.

In recent years, several attempts have been made to develop powder feeder systems in DMD processes. Gruenenwald, [4] designed a powder feeding system for the requirements of laser surface treatment. Yang, [14] [7] developed a powder feeder for large area laser cladding. Mei, [10] developed a new powder feeder system based on the weight base control system. Yang and Evans [13] worked to review the metering and dispensing of powder for free-form fabrication methods. They mentioned powder dispensing methods like vibration methods, electrostatic methods, screw/auger methods, pneumatic methods, and volumetric methods.

A wheel feeder [11] system employed in the DMD laser aided manufacturing process has closed loop electrical controls in order to have precise, repeatable, and reliable powder metering. This powder feeder system has an interface with a Programmable Logic Control (PLC) that allows remote control operation. The feedback motor provides precise and consistent motor speed. As this feeder is made traditionally for laser cladding applications, mass flow rate is high. The wheel feeder has a wheel that has indexing slots. Powder flows to the bottom of the wheel through indexing holes. Figure 1.2 illustrates the commercial wheel feeder system used in laser cladding applications.

Figure 1.2. Commercial Wheel Feeder used for Thermal Spraying Applications

In the next chapter, a detailed explanation of perturbation frequency and performance metric is discussed. Chapter three contains experiments designs, experimental setup, data analysis designed to test the significance of the performance metric with deposit quality, data validation and comparison of the disk feeder with wheel feeder. Chapter four concludes this study.

2. INTRODUCTION TO PERFORMANCE METRIC

2.1. PERTURBATION FREQUENCY

Achieving a consistent mass flow rate is essential for a good quality DMD process. However, no powder feeder system has a coherent mass flow when the resolution of the mass flow rate is magnified. This inconsistency can be from different parameters. Some of the factors are powder feeder design, powder properties, and motor controls. Perturbation frequency of powder feeder systems is defined as the disturbances in the mass flow pattern due to feeder system designs, the poor powder flow properties, or inconsistent motor controls. Inconsistencies in flow from the powder feeder design can be from feed mechanism used. Powder flow properties can include the irregular size of powder particles, and powder flowability. Inconsistent motor controls lead to perturbations in powder flow.

2.1.1. Mass Flow Patters. This study focuses on perturbation frequencies from the powder feeder design. Different mass flow cases are considered and studied to understand perturbation frequency. The same amount of mass is considered, for all the flow cases. The second section deals with perturbation frequencies from inherent powder feeder designs.

- **Inconsistent Mass Flow Pattern - Case 1.** This case arises when the powder feeder is inconsistent in its operation. The mass flow rate is inconsistent with respect to the powder feeder and laser deposition systems. The mass flow rate varies in a non-uniform fashion Figure 2.1 illustrates this below. Each sphere represents powder packets. Distance between lines represents melt pool diameter. Powder flow starts second melt pool diameter and ends at seventh melt pool diameter distance. There is no powder flow throughout the substrate. This case arises due to improper setting to the system.

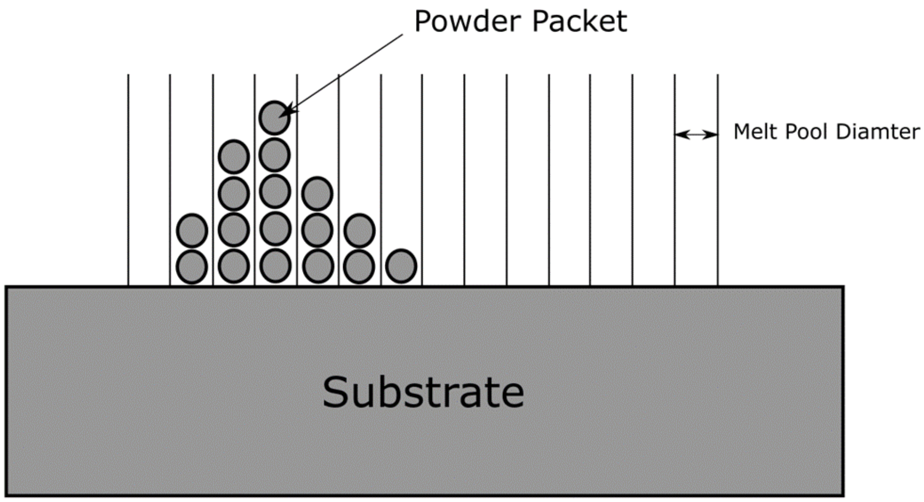

Figure 2.1. Representation of Powder Packets per Melt Pool Diameter Lengths along the Length of Substrate for Inconsistent Mass Flow Pattern - Case 1

- **Inconsistent Mass Flow Pattern - Case 2.** This case arises when the powder feeder is consistent in its operation. The mass flow rate is compatible with respect to the powder feeder but not to the laser deposition system. This flow pattern is the most common in all the powder feeder systems. The mass flow rate pattern is illustrated in Figure 2.2. Perturbations in mass flow are due to inherent powder feeder system designs or inconsistent motor controls. The substrate figure illustrates that perturbations in mass flow were observed over the entire duration. Mass flow reached a maximum and fell over consistent intervals.

- **Consistent Mass Flow Pattern.** A consistent mass flow pattern is difficult to achieve as it is an ideal case. The mass flow rate is constant to both the powder feeder and

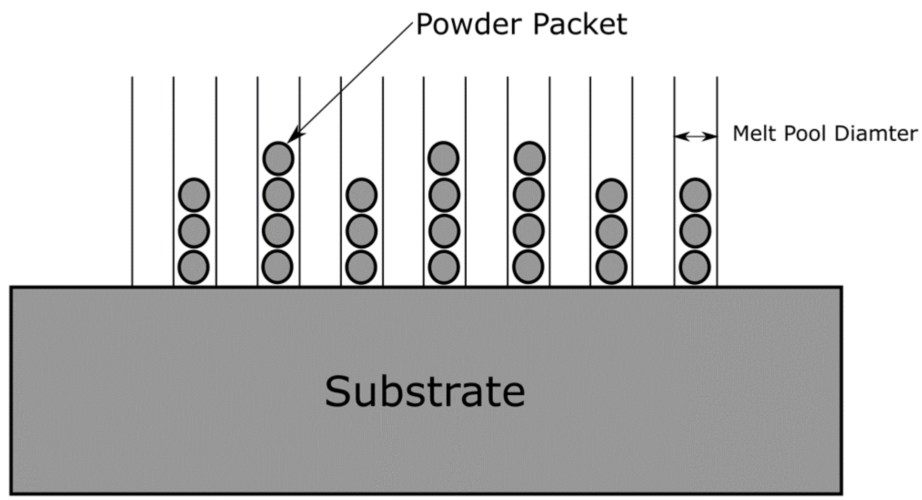

Figure 2.2. Representation of Powder Packets Unevenly Distributed per Melt Pool Diameter Lengths along the Length of Substrate for Inconsistent Mass Flow Rate - Case 2

the laser deposition system. Mass flow rate is over the given duration of time was consistent. In Figure 2.3 for each melt pool diameter, consistent number of powder packets are delivered by the powder feeder system. For a good quality deposit the flow pattern should be similar.

2.1.2. Powder Feeder Designs. This study focused on perturbations in mass flow due to the mechanical design parameters of the powder feeder systems. Due to design flaws, perturbation frequencies were observed in mass flows. Three prominent powder feeder system designs were considered. Screw design, wheel design and disk design were studied. Each design of the feed mechanism system is explained thoroughly.

- **Screw Feeder Systems.** Screw feeder systems are the first generation designs used for low powder flow rates in the DMD process. Powder from the hopper is delivered into a rotating horizontal screw with uniform threads. The mechanism is illustrated

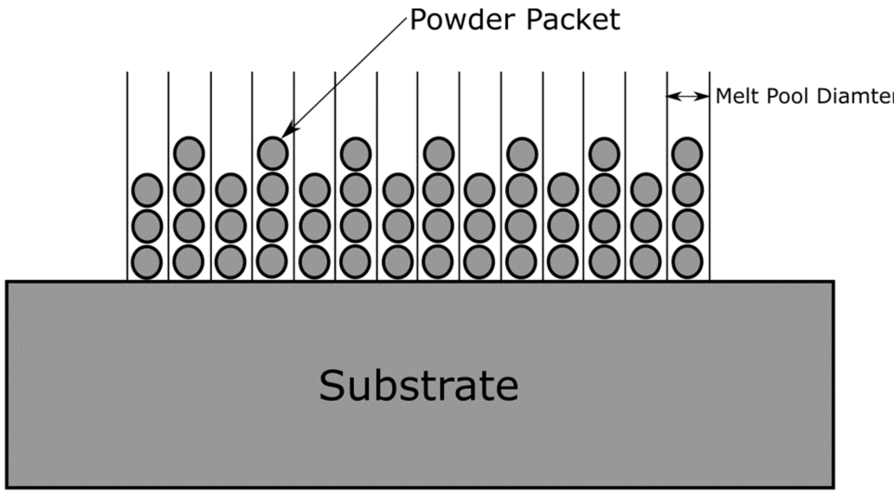

Figure 2.3. Representation of Powder Packets Evenly Distributed per Melt Pool Diameter Lengths along the Length of Substrate for Consistent Mass Flow Rate

in Figure 2.4. Powder on the rotating threads is carried forward as the screw rotates. Once the powder reaches the tip of the screw, it is transferred down and feeds into the deposition system. Powder on the rotating thread is delivered as powder packets or batches. Perturbations in the mass flow are inherent in this design. The powder is delivered inconsistently with respect to the laser deposition system. Perturbation frequency depends on the number of threads and the rotation speed of the screw. Various components of the screw feeder system include a hopper, a screw feed system, and motor controls. The hopper system attaches to the screw feeder system.

- **Wheel Feeders Systems.** Most laser cladding and laser spraying operations use wheel feeder systems. Powder from the hopper is delivered to the laser deposition system by a rotating index wheel in the powder feeder. The index wheel rotates the motor shaft on the motor. Holes on the index wheel are calibrated accordingly. Carrier gas runs in and carries powder out through one part of the index wheel, as illustrated in Figure 2.5. There is a significant distance between the holes on the

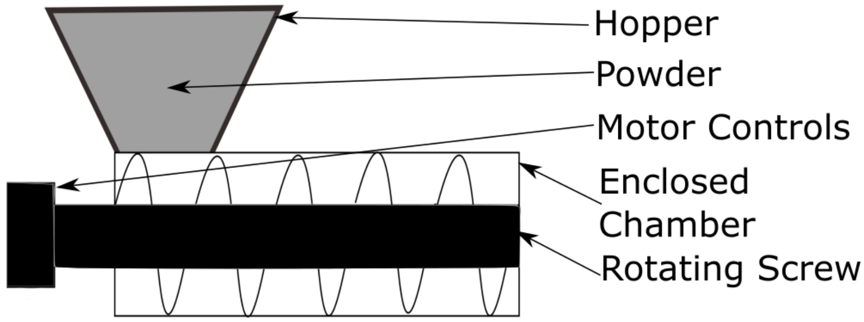

Figure 2.4. Schematic Representation of Screw Feeder Used in Blown Powder Metal Deposition has Inherent Perturbations in Powder Flow from its Rotating Screw Design

index wheel. The powder delivers is delivered as packets rather than a continuous stream. The mass flow pattern resembles Figure 2.2. The perturbations in this design are inherent from the powder feeder system design. The perturbation frequency for the design is the ratio of the total number of holes on the index wheel to the speed of the index wheel. The feeders is for high mass flow rate applications. Components of the wheel feeder system consist of a hopper, an indexing wheel system, a flow system for powder and gas, and motor controls. The indexed wheel system attaches to the motor shaft and sits at the bottom of the hopper as shown.

- **Disk Feeders Systems.** Disk feeder systems have low mass flow rates and more precision for the DMD process. The disk feeder system has a simple mechanism. Powder flows from the hopper directly onto the rotating wheel. The rotating wheel has a continuous groove. Powder flows from the hopper into the groove on the rotating wheel. From the other end carrier gas carries the powder out from the groove on the rotating wheel. This mechanism is illustrated in Figure 2.6. The entire system is enclosed in a closed pressurized chamber. As powder runs onto the wheel, it is delivered in a continuous flow. The powder flow rate has no inherent mechan-

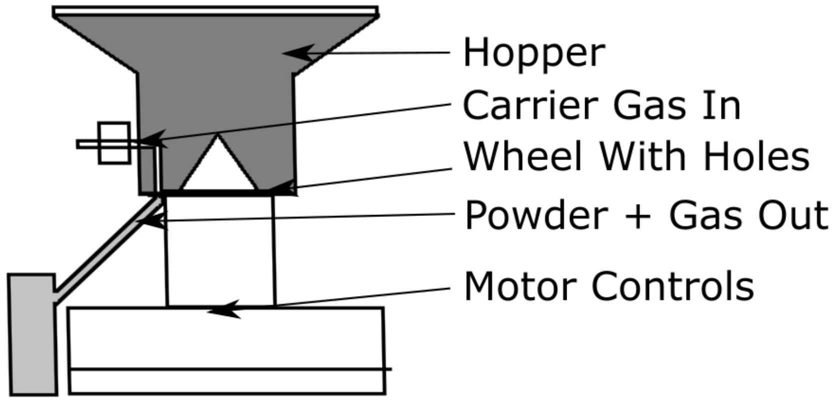

Figure 2.5. Schematic Representation of Wheel Feeder used in Blown Powder Metal Deposition has Inherent Perturbations in Powder Flow from its Rotating Wheel Design

ical perturbations from this powder feeder design. This design has no perturbation frequencies in the mass flow from the redundant system design. The mechanism depends on the resolution of motor controls. The powder is delivered in a continues flow. The mass flow pattern resembles the flow pattern in Figure2.3. No perturbations in the mass flow rate were observed for this redundant design. The disk feeders components include a hopper system, a rotating disk system, motor controls and an enclosure system. The enclosure system is used to pressurize the entire system to move the powder.

From the motor controls point of view, delay in the motor controls leads to perturbations in mass flow rate due to motor controls. If the motor is full of metal powder, it functions improperly and leads to perturbations in motions. Disk feeder systems are chosen to study the perturbation frequency concept and to establish the performance metric. Disk feeder has no perturbation frequencies inherent from their design. while working with the disk feeders, perturbations are induced into the system with the help of microcontrollers.

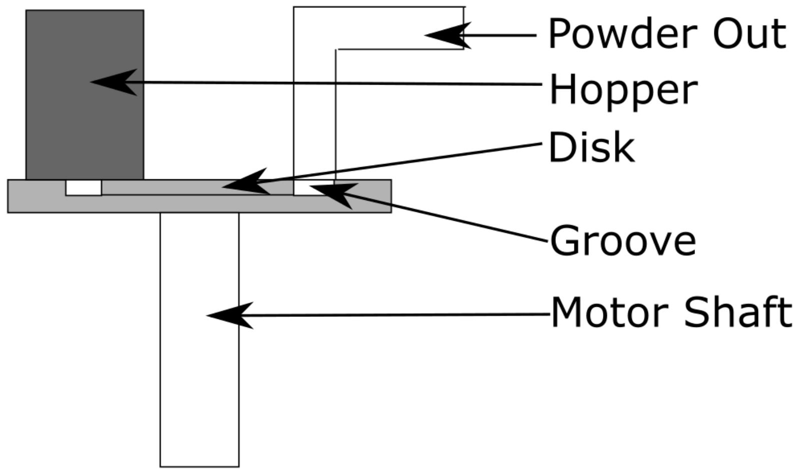

Figure 2.6. Schematic Representation of Disk Feeder used in Blown Powder Metal Powder Deposition, has No Known Perturbations in Powder Flow from its Design

2.2. ALGORITHM FOR PERFORMANCE METRIC

2.2.1. Laser Deposition System. The deposition frequency is the rate at which the deposition system moves over time with respect to the melt pool. It is denoted as $Frequency_{Deposition}$ and measured in Hertz. The equation for the system's frequency of deposition is

$$Frequency_{Deposition} = \frac{Diameter_{Melt\,Pool}}{Scan\,Speed\,of\,Laser} \tag{2.1}$$

A laser system has a CNC table that moves at a particular rate. The feed rate is the distance traveled in the x-y plane per unit of time. The diameter of melt pool is the measure of the spot size of the laser system. Values of the melt pool vary with power and scan speed.

2.2.2. Powder Feeder System Frequency. Disk feeder systems are designed to determine the perturbation frequency. This design, when compared with other designs, has fewer perturbations in the mass flow rate. Internal perturbations are hard to find. In the system, perturbations were introduced to determine the performance metric. Arduino was used to induce perturbations to the motor controls system of the disk feeder. The powder feeder system frequency is denoted by $Frequency_{Feeder}$ and measured in Hertz.

$$Frequency_{feeder} = \frac{No.of\,Perturbations\,per\,Revolution}{Time\,for\,one\,Rotation} \tag{2.2}$$

2.2.3. Performance Metric. The performance metric for powder feeder systems in additive manufacturing determines the error in powder flow rate and the performance of the feeders. The performance metric is denoted as P_{metric}. It ranges from zero to infinity with zero being the worst deposit and infinity being the best deposit. The equation for the frequency of the deposition system is

$$P_{metric} = \frac{Frequency_{Feeder}}{Frequency_{Deposition}} \tag{2.3}$$

3. RESULTS

3.1. TESTING PERFORMANCE METRIC

This study is done to test the performance metric with various laser scan speeds and mass flow rates. All the process parameters like the powder flow rate per unit length, carrier gas flow rate, laser power density per unit length, and melt pool diameter were kept constant. A disk feeder was used for these experiments. As the performance metric depends on both perturbation frequency and laser system frequency, change in the laser system frequency changes the perturbation frequency. All the above parameters are shown in Table 3.1

Setting Perturbation Frequency: Perturbation frequency was calculated after considering all the process parameters. The perturbation frequency was adjusted to the servo drive motor control with the help of a microcontroller. The microcontroller sent inputs to the servo driver with the assistance of a personal computer. The powder flow rate was initially set. The later amplitude for the perturbation frequency was set. Finally, the perturbation frequency that was already calculated from the process parameters was adjusted to the servo driver by the microcontroller. After all these settings were made the powder feeder system was turned on.

Design of Experiments: Experimental tests were conducted to test the significance of the performance metric with the quality of the deposit. The perturbation frequency was for laser scan speeds of 100 and 300 millimeter per minute. The melt pool diameter, powder flow per unit length, and laser power density were taken as two millimeters, five

Table 3.1. List of all the Process Parameters Considered for Testing Significance of Performance Metric

Process Parameter	Effecting Parameter	Value
Melt Pool Diameter	Laser System Frequency	1.7 - 2.6 mm
Laser Scan Speed	Laser System Frequency	100 to 300 mm per min
Laser Power	Laser System Frequency	260 to 770 watts
Powder Feeder Design	Perturbation Frequency	Disk Feeder
Volume of the Disk	Perturbation Frequency	1.5 cc
Powder Flow Rate	Perturbation Frequency	3, 5, 8 grams per min
Wheel Speed	Perturbation Frequency	5 rpm
Carrier Gas Flow Rate	Perturbation Frequency	40 scfh
Powder inuse	Perturbation Frequency	SS 316L
Apparent Density of Powder	Perturbation Frequency	4.2 grams per cc
Bulk Density	Perturbation Frequency	7.8 grams per cc
Packing Efficiency	Perturbation Frequency	4.16 grams per cc
Average Particle Size	Perturbation Frequency	85 microns (avg)

grams per cubic centimeters for 100 millimeters per minute laser scan speed. All the above parameters were kept constant. The objective of these experiments was to find the significance of surface roughness of the deposits, physical meaning, and range of the metric.

Treatment Structure: The treatment structure consisted of a two-way factorial arrangement. Two factors in this arrangement were the performance metric and the laser scan speed. The two factors had six and two levels, respectively, ranging from 0.01, 0.5, 1, 5, 20, and 70 for the performance metric and 100 and 300 millimeters per minute for the laser scan speed. The response variable was the normalized surface roughness of the deposit. The number of replications was two. The total number of experimental units was 24. Treatment structure is shown in Table 3.2.

Experimental Procedure: The powder feeder was filled with stainless steel 316 L powder. The apparent density of this powder was 4.12 grams/cc. The feeder was properly

Table 3.2. Treatment Structure showing Number of Factors and Number of Levels Considered for Testing Performance Metric

Factors	Number of levels
Performance Metric	6
Laser Scan Speed	2

closed by sealing the sight glass on the hopper. Motor connections were connected to the servo driver, microcontroller, and a personal computer. Powder outlet connections were connected from the powder feeder to the laser deposition system. Gas flow rate connections were adjusted. The gas flow rate was regulated by the flow meter. Stainless steel 316 Substrate was fixed onto the fixture table in the laser system. The volume around the substrate was enclosed with the shield gas argon. The powder feeder was turned on with the help of a microcontroller at a set perturbation frequency. Initially, the laser was shot on Ti64 substrate to remove its oxygen content. Later, the laser ran on the work-piece at respective scan speeds. The mass flow rate per unit length remained constant throughout the experiment. The gas flow rate for the powder feeder remained constant. The laser power density remained constant throughout the experiment. The experimental setup of the laser deposition system is shown in Figure 3.1.

Design Structure: Treatment combinations were randomized. As there were six levels of performance metric with two replications, there were 12 treatment combinations. All the treatment combinations were written on pieces of paper and put in a bowl. The pieces of paper were picked from the bowl randomly. Below figure gives the order in which experiments are conducted. In the below table L, R and M stand for laser scan speed 100 and 300, replications 1 and 2 and Metric 0.01, 0.5, 1, 5, 20 and 70 respectively. Order is shown in Table 3.3

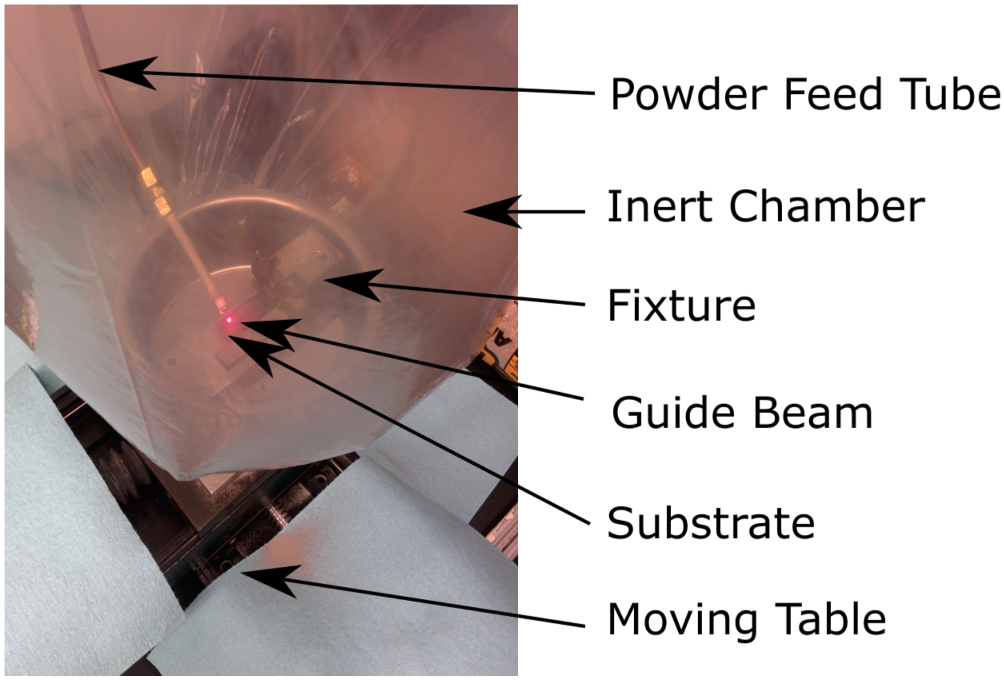

Figure 3.1. Experimental Setup of Laser Deposition System Used for Testing Significance of Scan Speed and Mass Flow Rate on the Performance Metric

Table 3.3. The Oder in which Experiments are Conducted for Testing Significance of Performance Metric

Order	Treatment Combination	Order	Treatment Combination
1	L2 R2 M6	13	L2 R1 M5
2	L1 R1 M2	14	L1 R1 M1
3	L1 R1 M3	15	L1 R2 M6
4	L2 R2 M4	16	L1 R2 M2
5	L2 R1 M6	17	L1 R1 M4
6	L1 R2 M2	18	L1 R1 M4
7	L2 R2 M1	19	L1 R1 M2
8	L1 R2 M5	20	L2 R1 M6
9	L2 R1 M5	21	L2 R2 M1
10	L2 R1 M3	22	L2 R2 M4
11	L2 R2 M3	23	L2 R2 M5
12	L1 R2 M1	24	L1 R1 M3

Laser Displacement Sensor: After the deposition process, all the deposits were scanned using a Keyence LK-G5000 laser displacement sensor. The schematic of the experimental setup is shown in the figure below. The substrate was fixed on a vise inside the Fadal 5 axis CNC machine. The laser displacement sensor head was fixed to the spindle of the CNC machine. The CNC program was written to scan the deposit at a constant feed rate over the entire deposit to avoid manually scanning the substrate. Data was logged for each deposit. This process was carried out for all the deposits. The experimental setup of the displacement sensor is shown in Figure 3.2

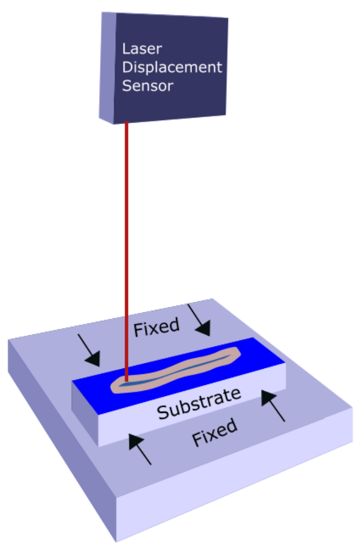

(a) Experimental Setup

(b) Laser Displacement Sensor

Figure 3.2. Experimental Setup of Laser Displacement Sensor Used for Measuring Surface Roughness of Depositions

Surface Roughness Values: Surface roughness along five-sixths of the deposited length was considered among all parameters to measure the quality of the deposit. Throughout the experiments, the deposition length was 30 millimeters. Starting and ending of the deposits were recessed. Parameters like the difference between the maximum and minimum height of the deposit were considered to measure the deposition quality.The mean height and surface roughness were calculated over two-thirds of the length of the deposit. The formula mentioned in 3.1 was applied to obtain surface roughness of the deposit.

$$R_a = \frac{1}{n}\Sigma^{n}{}_{i=1}|y_i| \tag{3.1}$$

Normalized Surface Roughness: All the calculated surface roughness values for each deposit were normalized to remove redundancy in the data. The surface roughness value was the mean of all the roughness values over the measured length. The normalized surface roughness value was the average of all individual normalized surface roughness values over the measured length. The individual normalized surface roughness equation is mentioned below. Normalized surface roughness is a good indicator of deposit quality Figure 3.3 shows an example to calculate normalized surface roughness. Final normalized surface roughness was the mean value of all the normalized surfaced values.

$$NR_a = \frac{R_a}{R_{max}} \tag{3.2}$$

The maximum normalized surface roughness measured while analyzing the deposits by the laser displacement sensor was 0.00168, and the minimum normalized surface roughness measured was 0.000404. Images of the deposits and respective surface roughness graphs for 100 mm/min laser scan speed and first replication experiment results are

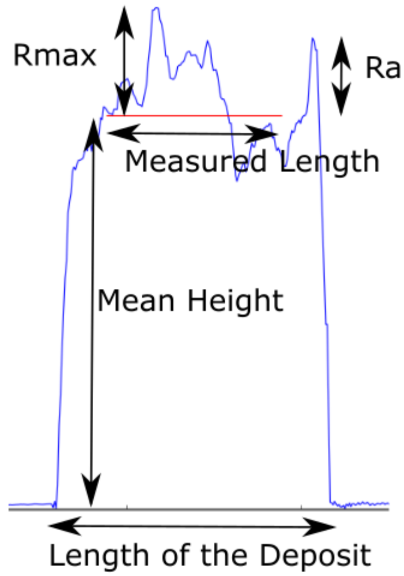

Figure 3.3. Sample Substrate Profile Measurement Graph to Interpret the Algorithm used to Calculation Normalized Surface Roughness over the Deposit Profile

shown. As the pictures show the roughness value decreased as the performance metric value increased. Figures 3.4 to 3.9 show the deposit quality for each respective performance metric. Figure 3.4 shows the mean height of the deposit was 1.224 mm and the normalized surface roughness was $1.689 * e^{-}03$. This was the highest roughness value among all the deposits. This deposit was inconsistent with no deposition in between. This deposit had a performance metric value of 0.01. Figure 3.5 mean height of the deposit was 0.53 mm. The normalized surface roughness is $1.441 * e^{-}03$. The deposit had three waveform patterns representing inconsistencies in powder flow. This deposit had a performance metric value of 0.5. Figure 3.6 shows the mean height of the deposit was 0.650 mm. The normalized surface roughness value is $1.159 * e^{-}03$. On the deposit, three patterns signifying inconsistencies in powder flow were observed. In the substrate profile, the measurement

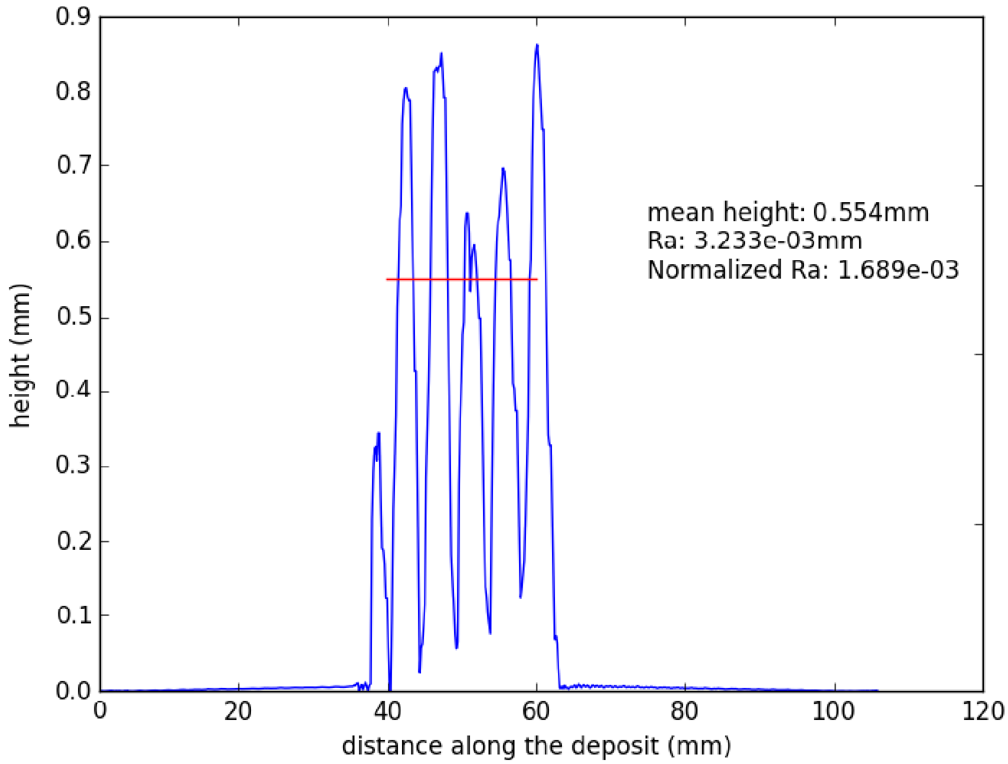

(a) Substrate Profile Height Measurement of the Deposit for Performance Metric 0.01

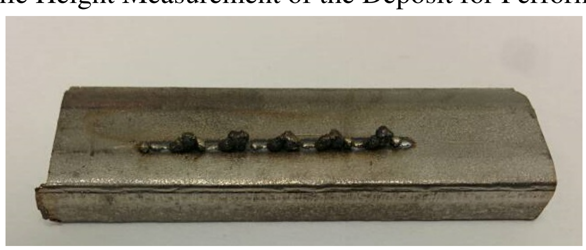

(b) Deposit Quality for Performance Metric Value of 0.01

Figure 3.4. Poor Deposition Quality for Performance Metric Value of 0.01, where the Deposit Quality is the Least

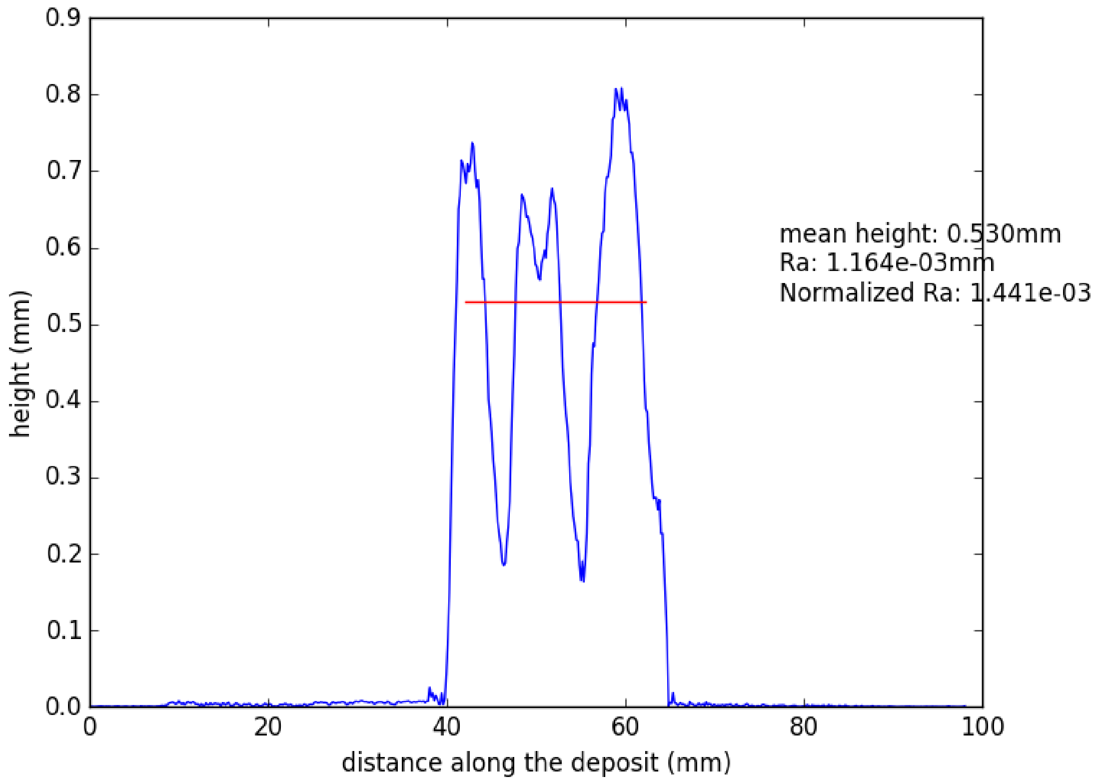

(a) Substrate Profile Height Measurement of the Deposit for Performance Metric 0.5

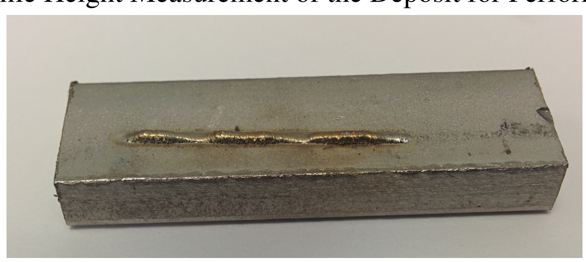

(b) Deposit Quality for Performance Metric Value of 0.5

Figure 3.5. Poor Deposition Quality for Performance Metric Value of 0.5, where the Deposit Quality is slightly Better than 0.01

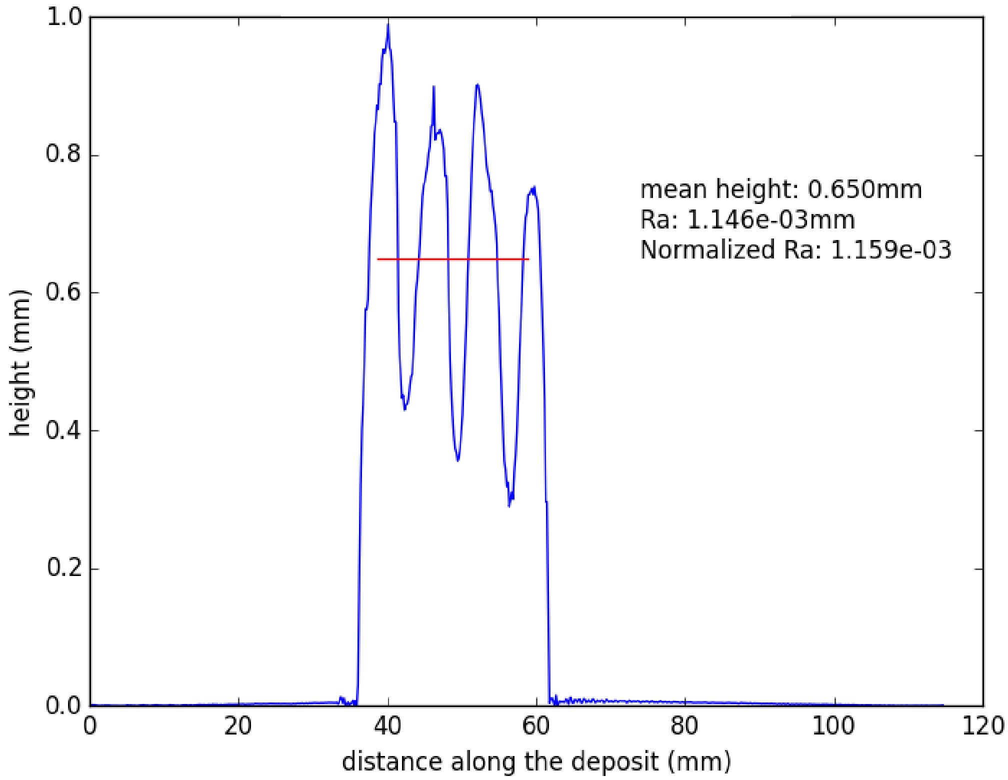

(a) Substrate Profile Height Measurement of the Deposit for Performance Metric 1

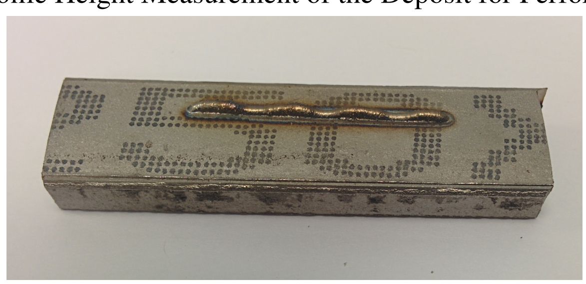

(b) Deposit Quality for Performance Metric Value of 1

Figure 3.6. Poor Deposition Quality refers to Performance Metric Value of 1, where the Deposit Quality is slightly Better than 0.5

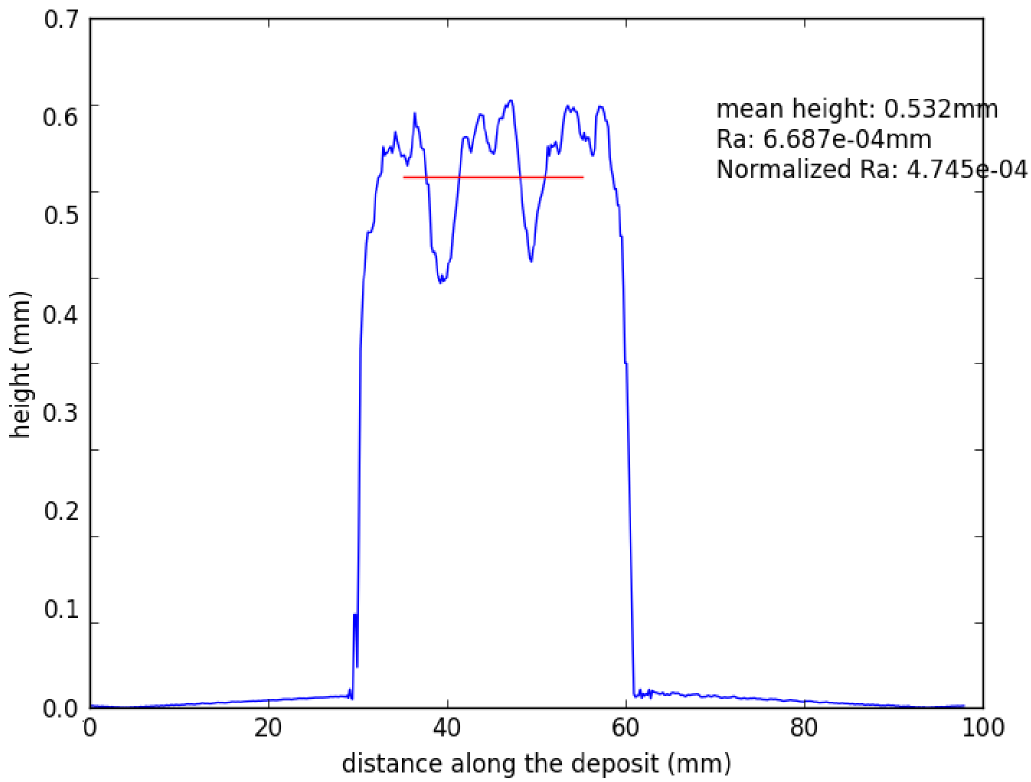

(a) Substrate Profile Height Measurement of the Deposit for Performance Metric 5

(b) Deposit Quality for Performance Metric Value of 5

Figure 3.7. Poor Deposition Quality refers to Performance Metric Value of 5 or Below

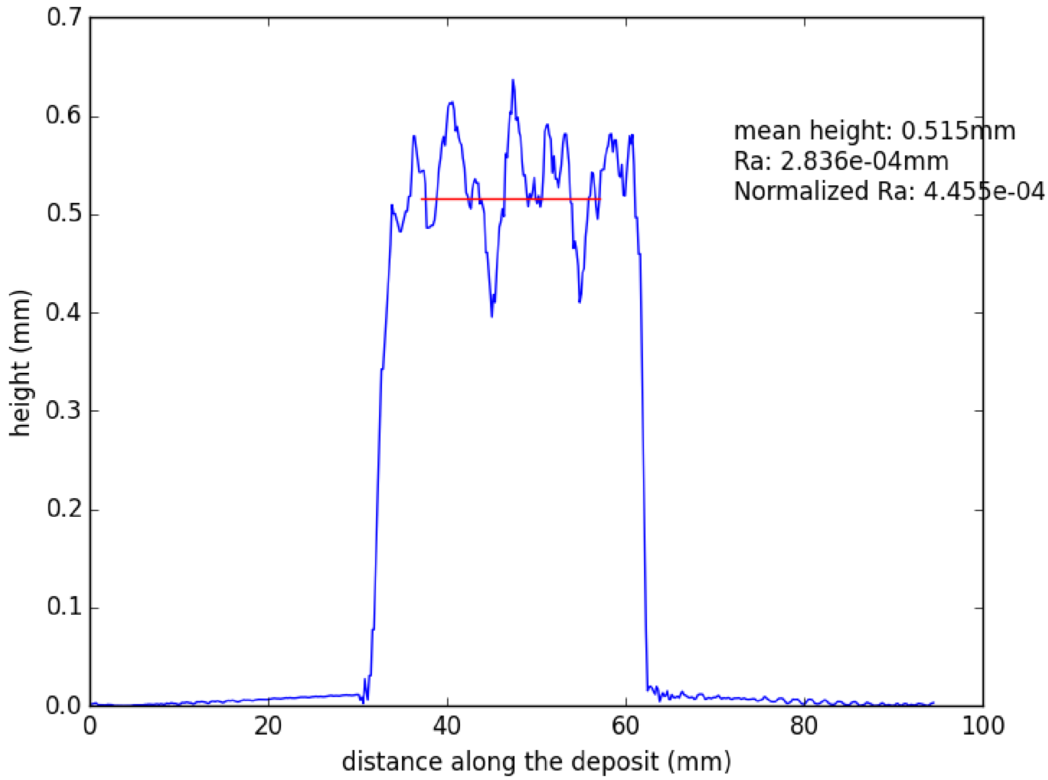

(a) Substrate Profile Height Measurement of the Deposit for Performance Metric 20

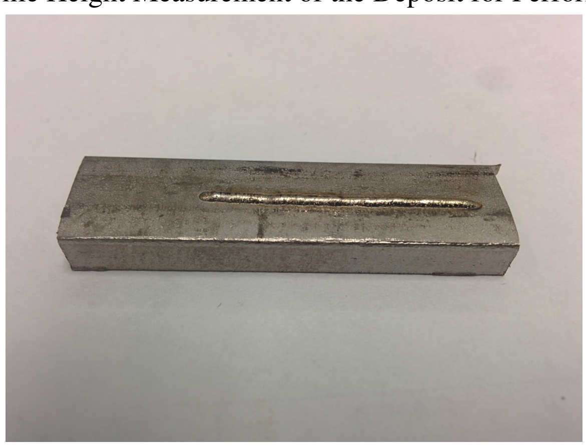

(b) Deposit Quality for Performance Metric Value of 20

Figure 3.8. Good Deposition Quality refers to Performance Metric Value of 20 or More

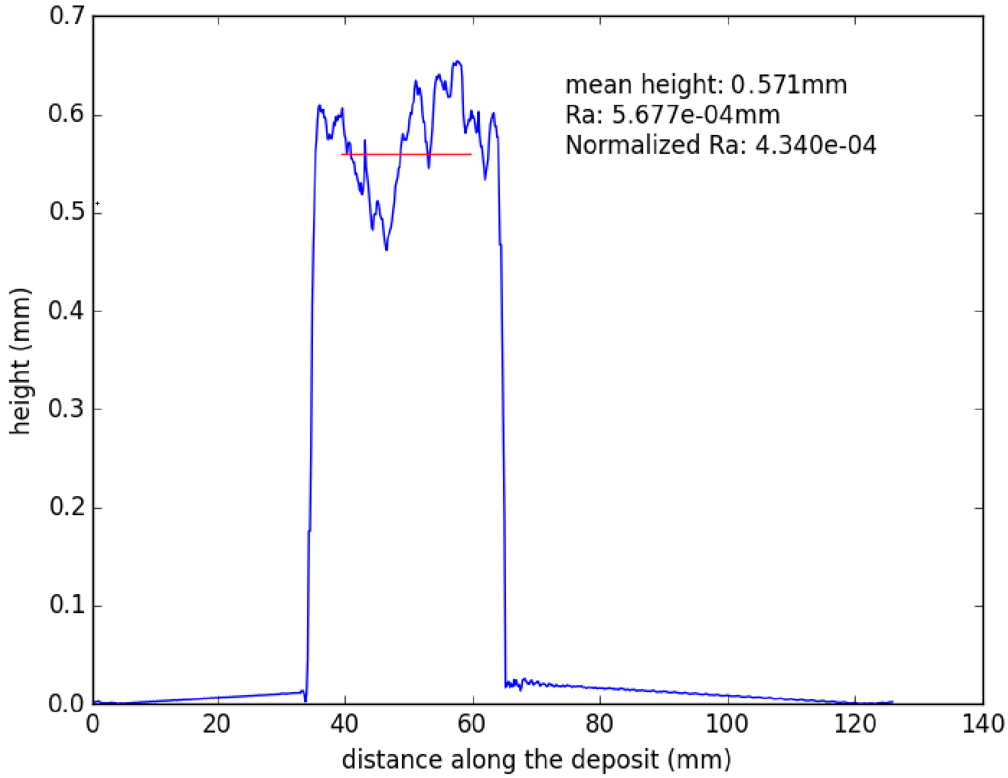

(a) Substrate Profile Height Measurement of the Deposit for Performance Metric 70

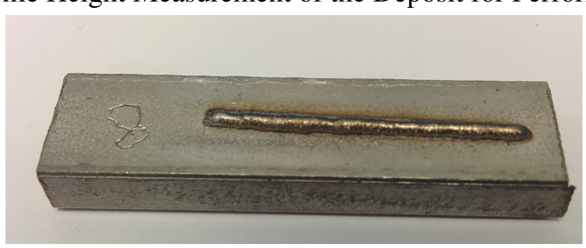

(b) Deposit Quality for Performance Metric Value of 70

Figure 3.9. Good Deposition Quality for Performance Metric Value of 70, where the Deposit Quality is Better than 20

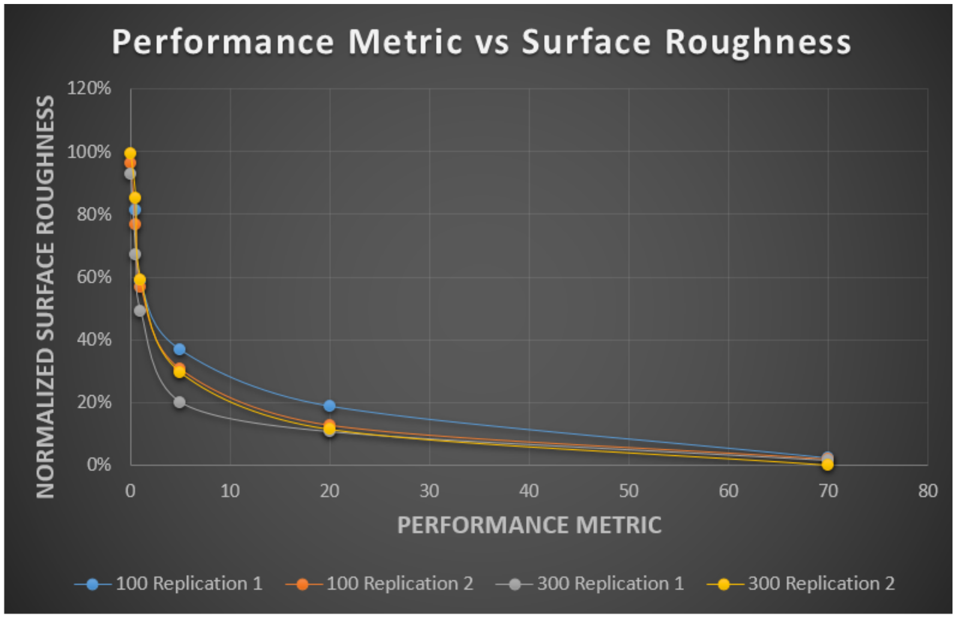

Figure 3.10. Comparison of Performance Metric and Normalized Data for Different Scan Speeds and Replications

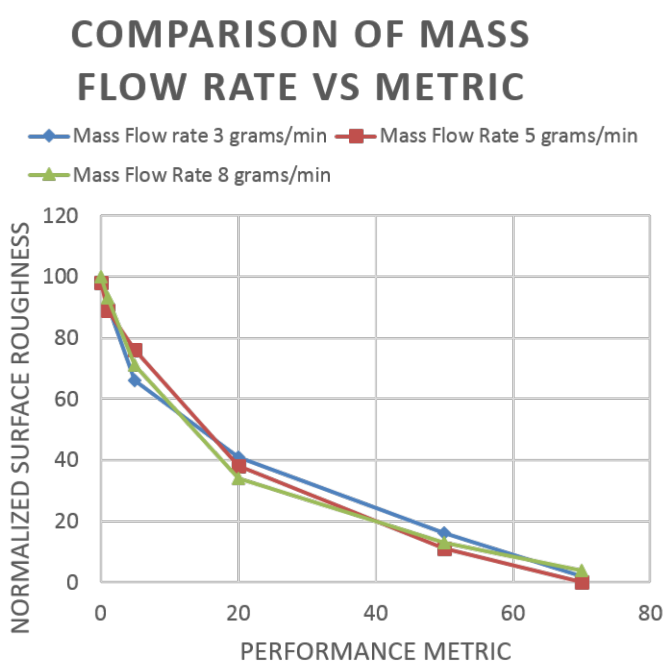

Figure 3.11. Comparison of Performance Metric and Normalized Data for Different Mass Flow Rates

graph patterns were observed. This deposit quality refers to a performance metric value of 1. Figure 3.7 show the mean height of the deposit was 1.232 mm. The normalized surface roughness value is $4.745 * e^{-}04$. The top view of the deposit is shown. The deposit had two less significant drops in the profile, leading to an increase in the normalized roughness value. The quality of the deposit refers to a performance metric value of 5. Figure 3.8 show the mean height was observed to 0.515 mm. The normalized surface roughness value was $2.836 * e^{-}04$. The deposit quality was better when compared to previous deposits. The quality of the deposit refers to a performance metric value of 20.

The fit model equation was used to validate the calculated model fit for the performance metric and surface roughness of the deposit. The model equation is

$$PredictedNormalizedRoughness = -0.00001111 * EstimatedMetric + 0.0008629 \quad (3.3)$$

Figure 3.9 show the mean height of the deposit was 1.21 mm. The normalized surface roughness value was $4.34 * e^{-}04$. The quality of the deposit refers to a performance metric value of 70. The motor controls were limited to only perturbation frequencies with metric value of up to 70. This study restricted the range of the performance metric to 70. These results show that the performance metric signified the quality of the deposit. All the experimental data is shown in Table 3.4. Two replications were done for both the scan speeds. The graph in the Figure 3.10 plotted with all the experimental data. the normalized data for the normalized surface roughness values was calculated. With the normalized data, all four experimental runs can be compared. Both the replications for 100 & 300 laser scan speeds were within the 5% deviation.

Table 3.4. Normalized Roughness Values for Different Performance Metric Values for Laser Scan Speeds of 100 and 300 mm/min

Sl Number	Laser Scan Speed (mm/min)	Replication	Performance Metric	Normalized Roughness Values	Normalized Data
1	100	1	0.001	0.00168	100%
2	100	1	0.5	0.00144	81%
3	100	1	1	0.00115	59%
4	100	1	5	0.00043	37%
5	100	1	20	0.00045	19%
6	100	1	70	0.00047	2%
7	100	2	0.001	0.00163	96%
8	100	2	0.5	0.00138	77%
9	100	2	1	0.00113	57%
10	100	2	5	0.00079	31%
11	100	2	20	0.00057	13%
12	100	2	70	0.00043	2%
13	300	1	0.001	0.00159	93%
14	300	1	0.5	0.00126	67%
15	300	1	1	0.00103	49%
16	300	1	5	0.00066	20%
17	300	1	20	0.00054	11%
18	300	1	70	0.00042	2%
19	300	2	0.001	0.00167	99%
20	300	2	0.5	0.00149	85%
21	300	2	1	0.00116	59%
22	300	2	5	0.00078	30%
23	300	2	20	0.00055	11%
24	300	2	70	0.0004	0%

3.2. VALIDATION OF THE MODEL

Normalized surface roughness was computed using given metric values. Predicted roughness values were calculated for a given metric value by varying the laser scan speed. Using the above equation 3.3 a predicted normalized roughness value is calculated for metric input value. In the validation experiments based on the metric values, the process parameters were determined.

Table 3.5. Comparison of Measured and Calculated Normalized Roughness Values for Validating the Predicted Model

Sl No	Scan Speed (mm/min)	Metric	Roughness Predicted	Roughness Measured	% Error
1	125	0.2	0.00086	0.00081	6%
2	125	10	0.00075	0.00079	-5%
3	125	25	0.00058	0.00057	2%
4	125	50	0.00030	0.00031	-2%
5	175	0.2	0.00086	0.00079	9%
6	175	10	0.00075	0.00074	2%
7	175	25	0.00058	0.00055	7%
8	175	50	0.00030	0.00029	5%
9	250	0.2	0.00086	0.00085	1%
10	250	10	0.00075	0.00073	3%
11	250	25	0.00058	0.00059	-2%
12	250	50	0.00030	0.00027	11%

Validation experiments with these process parameters were carried out. Surface roughness of the deposit was measured and compared with predicted values. Twelve sets of experiments were done to validate the fit model. The percentage error between measured and predicted normalized surface roughness values was calculated. A deviation range of -5% to 11% over the fit model was observed. Values mentioned below in the Table 3.5. Based on metric values, after determining the process parameters, three different and unknown scan speeds were used to validate the experiments. Scan speeds of 125, 175, and

250 millimeters per minute were considered. For all the experiments, the maximum deviation for a scan speed of 250 mm/sec was observed. The predicted normalized roughness values were compared with measured values for respective scan speeds. From the validation experiments, the predicted model was tested, and the deviation was observed to be less than 10%

3.3. WHEEL FEEDER AND DISK FEEDER COMPARISON

While comparing the wheel feeder with the new disk feeder, all the process parameters were kept constant. Only the scan speed was varied. Both the feeders had the same wheel speed, carrier gas flow rate, and powder. All the parameters of the laser deposition system were kept constant apart from the scan speed. Deposits were scanned under the laser displacement sensor to measure the normalized roughness values.

Table 3.6. Comparison of Normalized Surface Roughness Values for Wheel Feeder and Disk Feeder Systems for same Process Parameters

Serial Number	Laser Scan Speed	Powder Feeder System Feeder System	Measured Normalized Roughness	Predicted Metric
1	250	Wheel	0.00075	3.1
2	250	Wheel	0.00078	2.5
3	250	Disk	0.00041	13.8
4	250	Disk	0.00038	12.7

In Table 3.6, a performance metric for disk feeders was around four times more than that of the wheel feeder. The lowest measured metric for the wheel feeder was 2.5, and the highest measured metric was 3.1. For disk feeders under the same process parameters, the measured metrics were 13.8 and 12.7. Figures 3.12 shows the deposit quality of the disk feeders was better than that of the wheel feeders. The top deposits were from the wheel

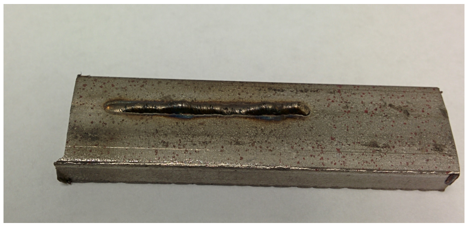

(a) First Deposit from Wheel Feeder System

(b) Second Deposit from Wheel Feeder System

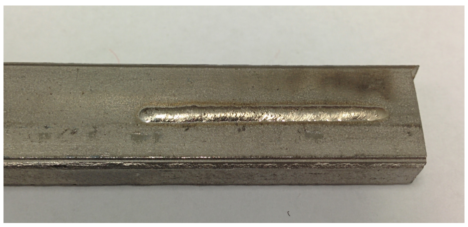

(c) First Deposit from Disk Feeder System

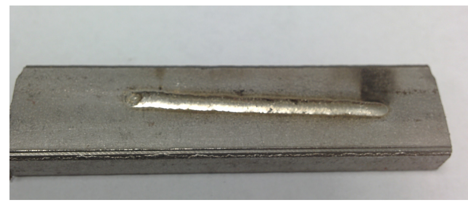

(d) Second Deposit from Disk Feeder System

Figure 3.12. Comparison of Deposition Quality from Wheel Feeder and Disk Feeder Systems at 250 mm/min Laser Scan Speed

feeder system, and the bottom deposits were from the disk feeder system. Without any external perturbation, the wheel feeders were observed to behave more inconsistently. The disk feeder had fewer inconsistencies than the wheel feeder.The disk feeder had a better performance metric over the wheel feeder system. Under the same process parameters, newly developed disk feeder had low normalized surface roughness values.

4. CONCLUSIONS

A detailed study on perturbation frequency by inherent powder feeder designs was conducted. Experiments were carried out to determine the significance between the measured surface roughness values of the deposits over theoretically calculated performance metric values. The results revealed the deposition quality and perturbations in the mass flow rate were significant and have no effect on laser scan speed mass flow rate. A quality deposit would be one whose performance metric value was 20 or greater. Validation experiments showed the data fit was significant. The wheel feeder and disk feeder were compared. The results showed a better performance metric for the disk feeder system under same process parameters. Based on these metrics, a feeder system can be chosen in future for production of functional graded materials (FGM).

BIBLIOGRAPHY

[1] S Chianrabutra, BG Mellor, and S Yang. A dry powder material delivery device for multiple material additive manufacturing.

[2] Todd M Francis, Christopher J Gump, and Alan W Weimer. Spinning wheel powder feeding deviceâĂŤfundamentals and applications. *Powder technology*, 170(1):36–44, 2006.

[3] Todd M Francis, Peter B Kreider, Paul R Lichty, and Alan W Weimer. An investigation of a fluidized bed solids feeder for an aerosol flow reactor. *Powder Technology*, 199(1):70–76, 2010.

[4] B Gruenwald, St Nowotny, W Henning, F Dausinger, and H Hugel. New technological developments in laser cladding. In *Laser Materials Processing*, volume 2306, page 934, 1994.

[5] BK Gullett and GR Gillis. Low flow rate laboratory feeders for agglomerative particles. *Powder technology*, 52(3):257–260, 1987.

[6] Pranav Kumar, James K Santosa, Elizabeth Beck, and Suman Das. Direct-write deposition of fine powders through miniature hopper-nozzles for multi-material solid freeform fabrication. *Rapid Prototyping Journal*, 10(1):14–23, 2004.

[7] L Li and WM Steen. Sensing, modeling and closed loop control of powder feeder for laser surface modification. *Laser Materials Processing*, 77:965–974, 1993.

[8] Xiaochun Li, Hongseok Choi, and Yong Yang. Micro rapid prototyping system for micro components. *Thin Solid Films*, 420:515–523, 2002.

[9] Shuji Matsusaka, Koji Yamamoto, and Hiroaki Masuda. Micro-feeding of a fine powder using a vibrating capillary tube. *Advanced Powder Technology*, 7(2):141–151, 1996.

[10] H Mei, M Valant, D Hu, and R Kovacevic. The characterization of the performance of a new powder feeder for laser based additive manufacturing.

[11] S Sampath, H Herman, N Shimoda, and T Saito. Thermal spray processing of fgms. *MRS bulletin*, 20(01):27–31, 1995.

[12] Takehiro Takano and Yoshiro Tomikawa. Excitation of a progressive wave in a lossy ultrasonic transmission line and an application to a powder-feeding device. *Smart materials and structures*, 7(3):417, 1998.

[13] S Yang and JRG Evans. Metering and dispensing of powder; the quest for new solid freeforming techniques. *Powder Technology*, 178(1):56–72, 2007.

[14] Xichen Yang, Xin Zhao, and Bao-Qi Wang. New development of laser cladding system on larger area for industrial application. In *Photonics China'96*, pages 14–19. International Society for Optics and Photonics, 1996.

VITA

Venkata Sivaram Bitragunta was born in Hyderabad, India. He received his Bachelor of Engineering (B.E) in Mechanical Engineering from Chaitanya Bharathi Institute of Technology, affiliated to Osmania University, Hyderabad, India in 2012. He has been pursuing his graduate studies in the Department of Mechanical and Aerospace Engineering at the Missouri University of Science and Technology (Formerly University of Missouri - Rolla) since July 2013. During his stay at Missouri University of Science and Technology, he held the position of Graduate Research Assistant. He received his Master of Science degree in Manufacturing Engineering from Missouri University of Science and Technology, Rolla, Missouri, the USA in December 2015.